Mechanics Research Communications 55 (2014) 59–65

Contents lists available at ScienceDirect

Mechanics Research Communications

journal homepage: www.elsevier.com/locate/mechrescom

Heat conduction analysis of laminated shells by a sampling surfaces method

G.M. Kulikov*, S.V. Plotnikova

Department of Applied Mathematics and Mechanics, Tambov State Technical University, Sovetskaya Street, 106, Tambov 392000, Russia

ARTICLE INFO

Article history:
Received 8 March 2013
Received in revised form 8 October 2013
Accepted 14 October 2013
Available online 30 October 2013

Keywords:
Heat conduction
Exact 3D analysis
Cross-ply composite shell
Angle-ply composite shell
Sampling surfaces method

ABSTRACT

A paper focuses on the use of the method of sampling surfaces (SaS) for the exact three-dimensional (3D) heat conduction analysis of laminated orthotropic and anisotropic shells. This method is based on selecting inside the nth layer I_n not equally spaced SaS parallel to the middle surface of the shell in order to choose the temperatures of these surfaces as basic variables. Such an idea permits the representation of the proposed thermal laminated shell formulation in a very compact form. The SaS are located inside each layer at Chebyshev polynomial nodes that improves the convergence of the SaS method significantly. As a result, the SaS method can be applied efficiently to exact 3D solutions of the steady-state heat conduction problem for cross-ply and angle-ply composite shells with a specified accuracy using a sufficient number of SaS.

1. Introduction

Nowadays, it is well established that for the accurate analysis of quasi-static thermoelasticity and thermopiezoelectricity problems for orthotropic and anisotropic laminated plates and shells it is necessary to solve the Fourier heat conduction equation because no prescribed through-thickness temperature distributions can be utilized (see, e.g. Tungikar and Rao, 1994; Savoia and Reddy, 1995; Soldatos and Ye, 1995; Kapuria et al., 1997; Tauchert et al., 2000; Vel and Batra, 2001, 2003; Brischetto, 2009; Brischetto and Carrera, 2011). This means that any algorithm for the numerical solution of the Fourier heat conduction equation must be incorporated in advanced computational models developed for the thermal stress analysis of laminated composite shells of arbitrary geometry and general layup configurations (Noor and Burton, 1992; Reddy, 2004). However, it is not a simple task because we deal here with the partial differential equation with variable coefficients depending on the thickness coordinate and many nodes in the thickness direction can be required to find the reliable results for thick shells.

To solve such a problem efficiently, we invoke the method of sampling surfaces (SaS) developed recently for the exact three-dimensional (3D) stress analysis of elastic and piezoelectric laminated plates (Kulikov and Plotnikova, 2012b, 2013a) and shells (Kulikov and Plotnikova, 2013b, 2013c). As SaS denoted by $\Omega^{(n)1}$, $\Omega^{(n)2}$, …, $\Omega^{(n)I_n}$, we select outer surfaces and any inner surfaces inside the nth layer in order to introduce the temperatures $T^{(n)1}$, $T^{(n)2}$, …, $T^{(n)I_n}$ of these surfaces as basic shell variables, where I_n is the number of SaS chosen for each layer ($I_n \geq 3$). This choice of temperatures with the consequent use of Lagrange polynomials of degree $I_n - 1$ in the thickness direction for each layer permits the representation of the governing equations in a very compact form. It is important that the developed approach with the arbitrary number of *equally spaced* SaS inside the shell body (Kulikov and Plotnikova, 2011a, 2011b) does not work properly with Lagrange polynomials of high degree because the Runge's phenomenon can occur, which yields the wild oscillation at the edges of the interval when the user deals with any specific functions. If the number of *equispaced* nodes is increased then the oscillations become even larger. Fortunately, the use of Chebyshev polynomial nodes (Kulikov and Plotnikova, 2012b, 2013c) can help to improve significantly the behavior of Lagrange polynomials of high degree for which the error will go to zero as $I_n \to \infty$.

An idea of using the SaS can be traced back to contributions of Kulikov (2001), and Kulikov and Carrera (2008) in which three, four and five *equally spaced* SaS are utilized. It is necessary to mention that in a layerwise differential quadrature (LWDQ) analysis (Liew et al., 2002, 2003; Zhang et al., 2003; Malekzadeh, 2009; Malekzadeh et al., 2008; Setoodeh et al., 2011) the nodal surfaces inside the mathematical layer are introduced following the general layerwise concept (Reddy, 2004; Carrera, 2003). The main difference consists in the lack of possibility to employ the Lagrange polynomials of high degree in the thickness direction. This is due to the fact that in a conventional LWDQ formulation only *equally spaced* nodal surfaces inside the mathematical layer are admissible

* Corresponding author. Tel.: +7 475 271 3299.
E-mail addresses: gmkulikov@mail.ru, kulikov@apmath.tstu.ru (G.M. Kulikov).

0093-6413/$ – see front matter © 2013 Elsevier Ltd. All rights reserved.
http://dx.doi.org/10.1016/j.mechrescom.2013.10.018

with the use of the simplest Lagrange polynomials of first and second orders. The next feature of the LWDQ method is that each nodal surface is discretized into a set of grid points in both plane directions. This means that one deals here with a numerical technique. On the contrary, the SaS method can be used efficiently for analytical developments (Kulikov and Plotnikova, 2012b, 2013c) and numerical implementations in strong and weak forms (Kulikov and Plotnikova, 2011a, 2011b, 2012a) as well.

The same concerns the finite layer method (Cheung and Jiang, 2001), which is the most efficient semi-analytical method for the 3D analysis of simply supported plates and shells (Akhras and Li, 2007, 2010; Wu and Li, 2010; Wu and Chang, 2012; Wu and Kuo, 2013). In this method, the shell is divided into a number of finite layers. Within each finite layer, the trigonometric functions are employed for in-plane interpolations of displacements in a displacement-based formulation (Wu and Kuo, 2013) and additionally transverse stresses in a mixed formulation (Wu and Chang, 2012), whereas the lower-order Lagrange polynomials with *equispaced* nodal points are accepted for the interpolation in the thickness direction, i.e. the h-refinement is adopted. Thus, the difference between the SaS method and the finite layer method consists in the following: the p-refinement is used in the former, while the h-refinement is used in the latter. Wu and his coauthors showed convincingly that the finite layer method with *equally spaced* nodal surfaces yields good predictions of the mechanical behavior of composite plates and shells. However, the 3D solutions derived are approximate. To obtain the exact 3D solutions, the p-refinement should be invoked. As pointed out earlier, the SaS method utilizes the Lagrange polynomials of high degree with Chebyshev polynomial nodes that allows one to minimize uniformly the error due to Lagrange interpolation. This fact gives an opportunity to find the exact 3D solutions for thermal laminated composite shells with a prescribed accuracy employing the sufficiently large number of SaS.

The present paper is intended to show that the SaS method can be applied efficiently to the exact solutions of some 3D steady-state problems of the heat conduction theory of laminated composite shells. The authors restrict themselves to finding five right digits in all examples presented except for a Section 4 with the results of the convergence study. The better accuracy is possible but requires more SaS inside each layer to be taken.

2. Description of temperature field

Consider a thick laminated shell of the thickness h. Let the middle surface Ω be described by orthogonal curvilinear coordinates θ_1 and θ_2, which are referred to the lines of principal curvatures of its surface. The coordinate θ_3 is oriented along the normal to the middle surface. Introduce the following notations: A_α are the coefficients of the first fundamental form of the middle surface; k_α are the principal curvatures of the middle surface; $\theta_3^{(n)i_n}$ are the transverse coordinates of SaS of the nth layer given by

$$\theta_3^{(n)1} = \theta_3^{[n-1]}, \quad \theta_3^{(n)I_n} = \theta_3^{[n]},$$
$$\theta_3^{(n)m_n} = \frac{1}{2}(\theta_3^{[n-1]} + \theta_3^{[n]}) - \frac{1}{2}h_n \cos\left(\pi \frac{2m_n - 3}{2(I_n - 2)}\right), \tag{1}$$

where $\theta_3^{[n-1]}$ and $\theta_3^{[n]}$ are the transverse coordinates of layer interfaces $\Omega^{[n-1]}$ and $\Omega^{[n]}$ depicted in Fig. 1; $h_n = \theta_3^{[n]} - \theta_3^{[n-1]}$ is the thickness of the nth layer; I_n is the number of SaS corresponding to the nth layer; the index m_n identifies the belonging of any quantity to the inner SaS of the nth layer and runs from 2 to $I_n - 1$, whereas the indices i_n, j_n, k_n to be introduced later for describing all SaS of the nth layer run from 1 to I_n; the index n identifies the belonging of any quantity to the nth layer and runs from 1 to N, where N is the total number of layers. Besides, the tensorial indices i, j range from 1 to 3 and Greek indices α, β range from 1 to 2.

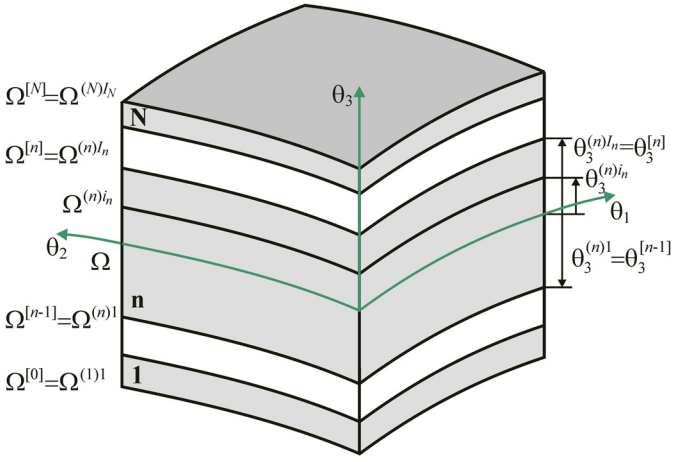

Fig. 1. Geometry of the laminated shell.

Remark 1. The transverse coordinates of inner SaS (1) coincide with the coordinates of Chebyshev polynomial nodes (Burden and Faires, 2010). This fact has a great meaning for a convergence of the SaS method (see, e.g. Kulikov and Plotnikova, 2012c).

The relation between the temperature T and the temperature gradient $\mathbf{\Gamma}$ is given by

$$\mathbf{\Gamma} = \nabla T. \tag{2}$$

In a component form, it can be written as

$$\Gamma_\alpha = \frac{1}{A_\alpha c_\alpha} T_{,\alpha}, \quad \Gamma_3 = T_{,3}, \tag{3}$$

where $c_\alpha = 1 + k_\alpha \theta_3$ are the components of the shifter tensor; the symbol $(\dots)_{,i}$ stands for the partial derivatives with respect to coordinates θ_i.

We start now with the first assumption of the proposed thermal laminated shell formulation. Let us assume that the temperature and temperature gradient fields are distributed through the thickness of the nth layer as follows:

$$T^{(n)} = \sum_{i_n} L^{(n)i_n} T^{(n)i_n}, \quad \theta_3^{[n-1]} \le \theta_3 \le \theta_3^{[n]}, \tag{4}$$

$$\Gamma_i^{(n)} = \sum_{i_n} L^{(n)i_n} \Gamma_i^{(n)i_n}, \quad \theta_3^{[n-1]} \le \theta_3 \le \theta_3^{[n]}, \tag{5}$$

where $T^{(n)i_n}(\theta_1, \theta_2)$ are the temperatures of SaS $\Omega^{(n)i_n}$ of the nth layer; $\Gamma_i^{(n)i_n}(\theta_1, \theta_2)$ are the components of the temperature gradient at the same SaS; $L^{(n)i_n}(\theta_3)$ are the Lagrange polynomials of degree $I_n - 1$ defined as

$$T^{(n)i_n} = T(\theta_3^{(n)i_n}), \tag{6}$$

$$\Gamma_i^{(n)i_n} = \Gamma_i(\theta_3^{(n)i_n}), \tag{7}$$

$$L^{(n)i_n} = \prod_{j_n \ne i_n} \frac{\theta_3 - \theta_3^{(n)j_n}}{\theta_3^{(n)i_n} - \theta_3^{(n)j_n}}. \tag{8}$$

The use of relations (3), (4), (6) and (7) yields

$$\Gamma_\alpha^{(n)i_n} = \frac{1}{A_\alpha c_\alpha^{(n)i_n}} T_{,\alpha}^{(n)i_n}, \tag{9}$$

$$\Gamma_3^{(n)i_n} = \sum_{j_n} M^{(n)j_n}(\theta_3^{(n)i_n}) T^{(n)j_n}, \tag{10}$$

where $c_\alpha^{(n)i_n} = 1 + k_\alpha \theta_3^{(n)i_n}$ are the components of the shifter tensor at SaS of the nth layer; $M^{(n)j_n} = L_{,3}^{(n)j_n}$ are the derivatives of Lagrange polynomials, which are calculated at SaS as follows:

$$M^{(n)j_n}(\theta_3^{(n)i_n}) = \frac{1}{\theta_3^{(n)j_n} - \theta_3^{(n)i_n}} \prod_{k_n \neq i_n, j_n} \frac{\theta_3^{(n)i_n} - \theta_3^{(n)k_n}}{\theta_3^{(n)j_n} - \theta_3^{(n)k_n}} \quad \text{for} \quad j_n \neq i_n,$$
$$M^{(n)i_n}(\theta_3^{(n)i_n}) = -\sum_{j_n \neq i_n} M^{(n)j_n}(\theta_3^{(n)i_n}). \tag{11}$$

It is seen from Eq. (10) that the transverse component of the temperature gradient $\Gamma_3^{(n)i_n}$ is represented as a *linear combination* of temperatures of all SaS of the nth layer $T^{(n)j_n}$.

3. Variational formulation of heat conduction problem

The variational equation for the laminated shell can be written as

$$\delta J = 0, \tag{12}$$

where J is the basic functional of the heat conduction theory given by

$$J = \frac{1}{2} \iint_\Omega \sum_n \int_{\theta_3^{[n-1]}}^{\theta_3^{[n]}} q_i^{(n)} \Gamma_i^{(n)} A_1 A_2 c_1 c_2 d\theta_1 d\theta_2 d\theta_3 - \iint_{\bar\Omega} TQ_n \, d\Omega, \tag{13}$$

where $q_i^{(n)}$ are the components of the heat flux vector of the nth layer; Q_n is the specified heat flux on the boundary surface $\bar\Omega = \Omega^{[0]} + \Omega^{[N]} + \Sigma$, where Σ is the edge boundary surface of the shell.

Substituting the through-thickness distribution (5) in Eq. (13) and introducing heat flux resultants

$$R_i^{(n)i_n} = \int_{\theta_3^{[n-1]}}^{\theta_3^{[n]}} q_i^{(n)} L^{(n)i_n} c_1 c_2 \, d\theta_3, \tag{14}$$

one obtains

$$J = \frac{1}{2} \iint_\Omega \sum_n \sum_{i_n} R_i^{(n)i_n} \Gamma_i^{(n)i_n} A_1 A_2 d\theta_1 d\theta_2 - \iint_{\bar\Omega} TQ_n \, d\Omega. \tag{15}$$

Now, we accept the second assumption of the proposed thermal laminated shell formulation. Let the constitutive equations be the well-known Fourier's heat conduction equations:

$$q_i^{(n)} = -k_{ij}^{(n)} \Gamma_j^{(n)}, \quad \theta_3^{[n-1]} \le \theta_3 \le \theta_3^{[n]}, \tag{16}$$

where $k_{ij}^{(n)}$ are the components of the thermal conductivity tensor of the nth layer.

Inserting (16) in Eq. (14) and taking into account (5), we have

$$R_i^{(n)i_n} = -\sum_{j_n} \Lambda^{(n)i_n j_n} k_{ij}^{(n)} \Gamma_j^{(n)j_n}, \tag{17}$$

where

$$\Lambda^{(n)i_n j_n} = \int_{\theta_3^{[n-1]}}^{\theta_3^{[n]}} L^{(n)i_n} L^{(n)j_n} c_1 c_2 \, d\theta_3. \tag{18}$$

4. Exact solution for orthotropic cylindrical shell

In this section, we study a laminated orthotropic cylindrical shell. Let the middle surface of the shell be described by axial and circumferential coordinates θ_1 and θ_2. The edge boundary conditions of the shell are considered as

$$\Theta^{(n)} = 0 \quad \text{at} \quad \theta_1 = 0 \quad \text{and} \quad \theta_1 = L, \tag{19}$$

where L is the length of the shell; $\Theta^{(n)}$ is the temperature rise in the nth layer from the initial reference temperature T_0 defined as

$$\Theta^{(n)} = T^{(n)} - T_0. \tag{20}$$

To satisfy boundary conditions (19), we search the analytical solution of the problem by a method of double Fourier series expansion

$$\Theta^{(n)i_n} = \sum_{r=1}^{\infty} \sum_{s=0}^{\infty} \Theta_{rs}^{(n)i_n} \sin \frac{r\pi\theta_1}{L} \cos s\theta_2. \tag{21}$$

Substituting (21) in Eqs. (9), (10) and (15) and taking into account (17) and (20), one finds

$$J = \sum_{r=1}^{\infty} \sum_{s=0}^{\infty} J_{rs}(\Theta_{rs}^{(n)i_n}). \tag{22}$$

Invoking further the variational Eq. (12), the following system of linear algebraic equations of order $\sum_n I_n - N + 1$ is obtained:

$$\frac{\partial J_{rs}}{\partial \Theta_{rs}^{(n)i_n}} = 0. \tag{23}$$

The linear system (23) can be easily solved by a method of Gaussian elimination.

The described algorithm was performed with the Symbolic Math Toolbox, which incorporates symbolic computations into the numeric environment of MATLAB. This gives the possibility to derive the exact 3D solutions of the steady-state heat conduction problem for laminated orthotropic cylindrical shells with a specified accuracy.

As a numerical example, we consider a single-layer orthotropic cylindrical shell made of the graphite-epoxy composite with geometric parameters $R = 1$ m and $L = 4$ m, where R is the radius of the middle surface. The thermal conductivities of the composite are taken to be $k_{11} = 100k_0$ and $k_{22} = k_{33} = k_0$, where $k_0 = 0.5$ W/mK.

The shell is loaded on the top surface by the sinusoidally distributed heat flux, whereas the bottom surface is assumed to be heat-insulated, that is

$$q_3^{[N]} = q_0 \sin \frac{\pi\theta_1}{L} \cos 2\theta_2, \quad q_3^{[0]} = 0, \tag{24}$$

where $q_0 = 1$ W/m^2 and $N = 1$. To investigate the possibilities of the SaS method for finding the exact 3D solutions of the steady-state heat conduction problem, we introduce the dimensionless temperature rise as follows:

$$\bar\Theta = 100k_0\Theta(L/2, 0, z)/Lq_0, \quad z = \frac{\theta_3}{h}. \tag{25}$$

Table 1 lists the results of a convergence study by increasing the number of SaS and using the temperature rise (25) at the center of a shell. As it turned out, the SaS method provides ten right digits (in fact, the better accuracy is possible) for the temperature rise at the top surface of the thick cylindrical shell employing 21 inner SaS inside the shell body. It should be noted that here the bottom and top surfaces are not included into a set of the SaS because the use of Chebyshev polynomial nodes allows one to minimize uniformly the error due to Lagrange interpolation (see, e.g. Burden and Faires, 2010).

Table 1
Temperature rise at the center of a single-layer cylindrical shell.

I_n	$R/h=4$ $\bar{\Theta}(-0.5)$	$R/h=4$ $\bar{\Theta}(0.5)$	$R/h=10$ $\bar{\Theta}(-0.5)$	$R/h=10$ $\bar{\Theta}(0.5)$	$R/h=100$ $\bar{\Theta}(-0.5)$	$R/h=100$ $\bar{\Theta}(0.5)$
3	−0.124138663	−1.314234752	−0.367523097	−1.355741083	−6.229845552	−6.355053515
7	−0.018387704	−1.405068442	−0.360402412	−1.360053886	−6.229845805	−6.355053476
11	−0.018374318	−1.405064911	−0.360402398	−1.360053873	−6.229845805	−6.355053476
15	−0.018374328	−1.405064896	−0.360402398	−1.360053873	−6.229845805	−6.355053476
19	−0.018374330	−1.405064895	−0.360402398	−1.360053873	−6.229845805	−6.355053476
23	−0.018374331	−1.405064894	−0.360402398	−1.360053873	−6.229845805	−6.355053476
27	−0.018374331	−1.405064894	−0.360402398	−1.360053873	−6.229845805	−6.355053476
31	−0.018374331	−1.405064894	−0.360402398	−1.360053873	−6.229845805	−6.355053476

5. Exact solution for axisymmetric anisotropic cylindrical shell

In this section, we study the axisymmetric heat response of the laminated anisotropic cylindrical shell with boundary conditions (19). We search again the analytical solution of the problem by a method of Fourier series expansion

$$\Theta^{(n)i_n} = \sum_r \Theta_r^{(n)i_n} \sin\frac{r\pi\theta_1}{L}, \tag{26}$$

where r is the wave number along the axial direction.

Substituting (26) in Eqs. (9), (10) and (15) and allowing for (17) and (20), one obtains

$$J = \sum_r J_r(\Theta_r^{(n)i_n}). \tag{27}$$

Invoking the variational Eq. (12), we arrive at the system of linear algebraic equations

$$\frac{\partial J_r}{\partial \Theta_r^{(n)i_n}} = 0, \tag{28}$$

of order $\sum_n I_n - N + 1$. The linear system (28) is solved by a method of Gaussian elimination.

The described algorithm was performed with the Symbolic Math Toolbox. This permits the derivation of exact 3D axisymmetric solutions for laminated anisotropic cylindrical shells with a specified accuracy.

5.1. Three-layer cross-ply cylindrical shell covered with piezoelectric layers

A symmetric three-layer cylindrical shell with the stacking sequence [90/0/90] is composed of the graphite-epoxy composite and covered with polyvinylidene fluoride (PVDF) layers on its bottom and top surfaces. This means that a five-layer hybrid cylindrical shell [PVDF/90/0/90/PVDF] with ply thicknesses $[3h_0/8h_0/8h_0/8h_0/3h_0]$ is studied, where $h_0 = h/30$. The thermal conductivities of the graphite-epoxy are $k_{11} = 36.42$ W/mK, $k_{22} = k_{33} = 0.96$ W/mK and of the PVDF are $k_{11} = k_{22} = k_{33} = 0.24$ W/mK. The geometric parameters are taken to be $R = 1$ m and $L = 4$ m. Here, we consider the case of the imposed sinusoidal temperature distribution on the top surface of a shell, while the bottom surface is maintained at the reference temperature:

$$\Theta^{[N]} = \Theta_0 \sin\frac{\pi\theta_1}{L}, \quad \Theta^{[0]} = 0, \tag{29}$$

where $\Theta_0 = 1$K and $N = 5$.

Table 2
Temperature rise in a five-layer hybrid cylindrical shell at $x = 0.5$ and $z = 0.1$.

R/h	4	6	10	20	50	100
$I_n = 3$	0.23984	0.25108	0.25482	0.25403	0.25200	0.25106
$I_n = 5$	0.23984	0.25108	0.25482	0.25403	0.25200	0.25106
Kapuria	0.2398	0.2511	0.2548	0.2540	0.2520	0.2511

The data listed in Tables 2 and 3 show that the SaS method allows one to find the exact solution for thick laminated orthotropic cylindrical shell with a prescribed accuracy by using three SaS inside each layer. The comparison with a closed form solution of Kapuria et al. (1997) is also given, where the dimensionless coordinates $x = \theta_1/L$ and $z = \theta_3/h$ are introduced. Fig. 2 presents the distributions of the temperature and heat flux in the thickness direction for different values of the slenderness ratio R/h employing three SaS for each layer. These results demonstrate convincingly the high potential of the proposed thermal laminated shell formulation. This is due to the fact that the continuity conditions at layer interfaces for the transverse component of the heat flux are satisfied exactly utilizing the constitutive Eq. (16).

5.2. Three-layer angle-ply cylindrical shell

Consider next a three-layer angle-ply cylindrical shell with the stacking sequence [45/−45/45] and ply thicknesses $h_1 = h_3 = h/4$ and $h_2 = h/2$. The layers are made of the graphite-epoxy composite with the material properties presented in a previous section. The geometric parameters are chosen as $R = 1$ m and $L = 4$ m. The shell is subjected to the axisymmetric heat on the top surface, whereas the bottom surface is assumed to be heat-insulated, that is

$$\Theta^{[N]} = \Theta_0 \sin\frac{\pi\theta_1}{L}, \quad q_3^{[0]} = 0, \tag{30}$$

where $\Theta_0 = 1$K and $N = 3$.

Table 4 demonstrates again the high potential of the thermal laminated shell formulation for different slenderness ratios R/h. The logarithmic errors given in Table 5 help to assess the accuracy of fulfilling the boundary condition for the heat flux on the bottom surface of a shell. It is necessary to note that the proposed SaS method provides the monotonic convergence that is impossi-

Table 3
Temperature rise in a five-layer hybrid cylindrical shell at $x = 0.5$ and $z = 0.9$.

R/h	4	6	10	20	50	100
$I_n = 3$	0.73853	0.75018	0.75440	0.75390	0.75197	0.75106
$I_n = 5$	0.73853	0.75018	0.75440	0.75390	0.75197	0.75106
Kapuria	0.7385	0.7502	0.7544	0.7539	0.7520	0.7511

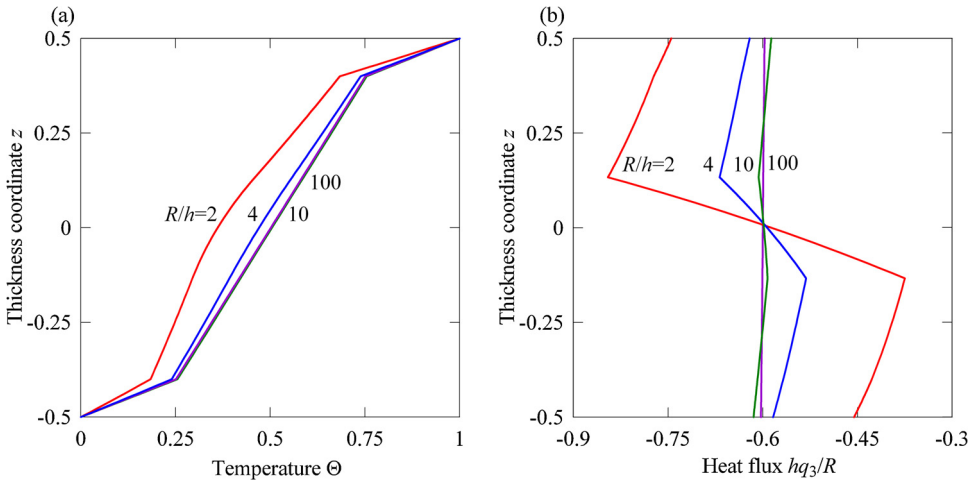

Fig. 2. Distributions of the temperature and heat flux through the thickness of the five-layer hybrid cylindrical shell at $x = 0.5$ for $I_1 = I_2 = I_3 = I_4 = I_5 = 3$.

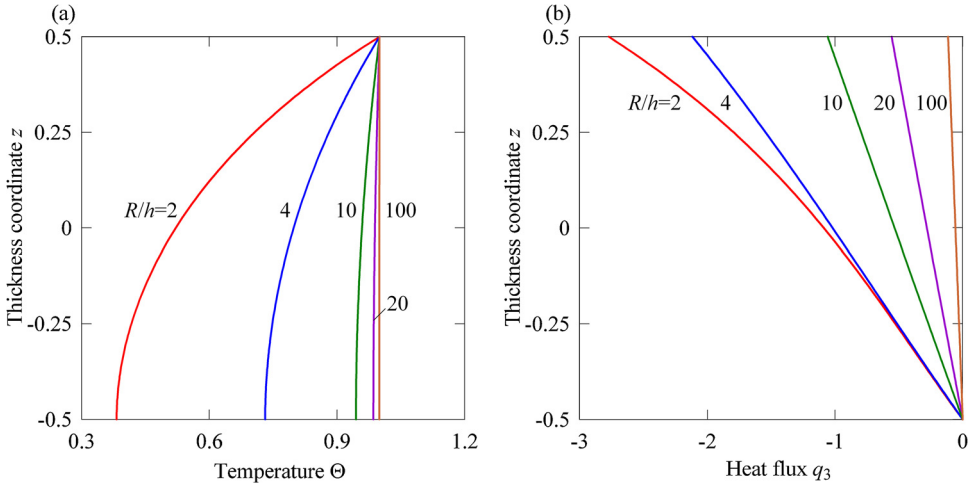

Fig. 3. Distributions of the temperature and heat flux through the thickness of the three-layer angle-ply cylindrical shell at $x = 0.5$ for $I_1 = I_2 = I_3 = 5$.

Table 4
Temperature rise in a three-layer angle-ply cylindrical shell at $x = 0.5$ and $z = 0$.

R/h	2	4	10	20	100
$I_n = 3$	0.52071	0.79787	0.95855	0.98908	0.99955
$I_n = 5$	0.52093	0.79789	0.95855	0.98908	0.99955
$I_n = 7$	0.52093	0.79789	0.95855	0.98908	0.99955

Table 5
Logarithmic error $lg\,|q_3|$ of fulfilling the boundary condition for the heat flux on the bottom surface of a three-layer angle-ply cylindrical shell at $x = 0.5$.

R/h	2	4	10	20	100
$I_n = 3$	−2.4962	−2.6748	−3.2890	−3.8510	−5.2259
$I_n = 5$	−4.6196	−5.5601	−7.0421	−8.2271	−10.653
$I_n = 7$	−7.2618	−8.8954	−10.966	−10.995	−10.385

ble with *equally spaced* SaS (Kulikov and Plotnikova, 2011a, 2011b). Fig. 3 displays the through-thickness distributions of the temperature and heat flux employing five SaS for each layer. It is seen that the continuity conditions for the heat flux at layer interfaces are satisfied again properly.

6. Exact solution for orthotropic cylindrical panel

Here, we study a laminated orthotropic cylindrical panel whose the middle surface is described by axial and circumferential coordinates θ_1 and θ_2. The edge boundary conditions are assumed to be

$$\Theta^{(n)} = 0 \quad \text{at} \quad \theta_1 = 0, a \quad \text{and} \quad \theta_2 = 0, b, \tag{31}$$

where a and b are the shell dimensions. To satisfy boundary conditions (31), we search the analytical solution of the problem by a method of double Fourier series expansion

$$\Theta^{(n)i_n} = \sum_r \sum_s \Theta_{rs}^{(n)i_n} \sin\frac{r\pi\theta_1}{a} \sin\frac{s\pi\theta_2}{b}, \tag{32}$$

where r and s are the wave numbers along axial and circumferential directions.

Inserting (32) in Eqs. (9), (10) and (15) and taking into consideration (17) and (20), we obtain

$$J = \sum_r \sum_s J_{rs}(\Theta_{rs}^{(n)i_n}). \tag{33}$$

The use of the variational Eq. (12) yields a system of linear algebraic equations

$$\frac{\partial J_{rs}}{\partial \Theta_{rs}^{(n)i_n}} = 0 \tag{34}$$

of order $\sum_n I_n - N + 1$. The linear system (34) is solved by a method of Gaussian elimination.

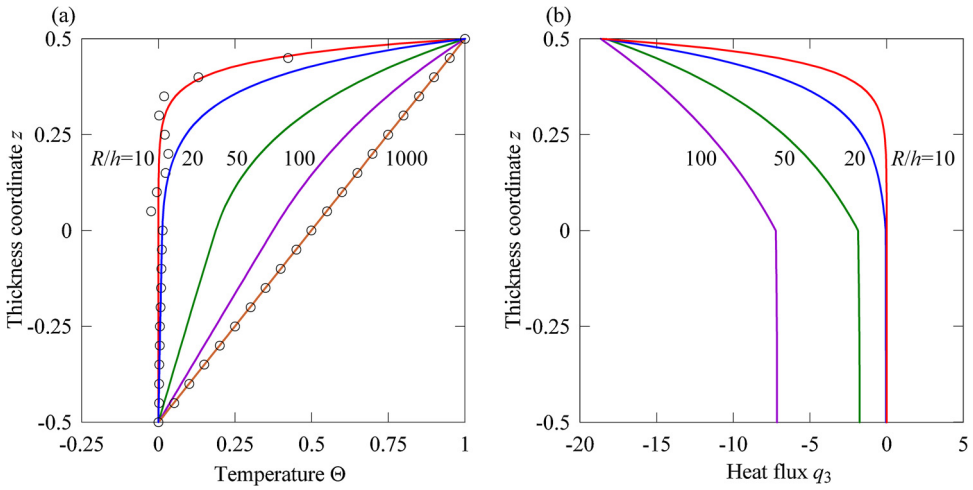

Fig. 4. Through-thickness distributions of the temperature and heat flux at the center of a two-layer cross-ply cylindrical panel for $I_1 = I_2 = 11$: present analysis (–) and Brischetto and Carrera (◯).

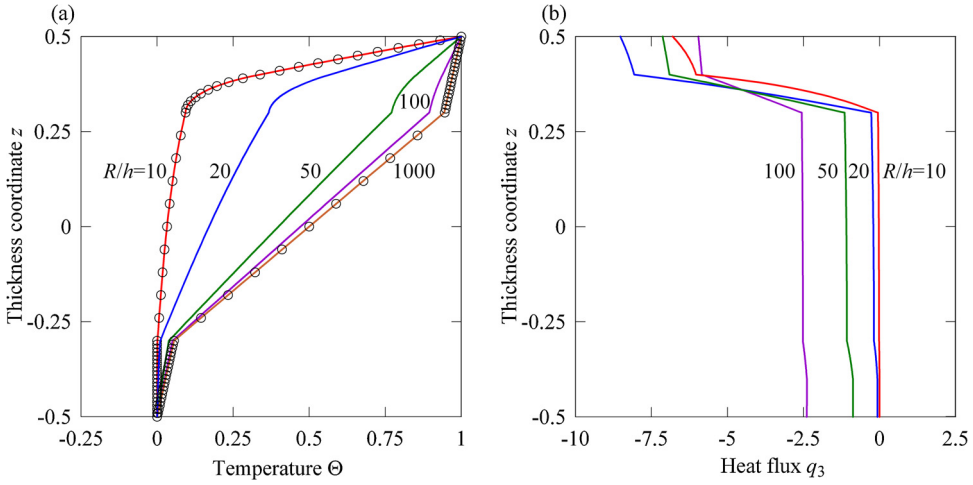

Fig. 5. Through-thickness distributions of the temperature and heat flux at the center of a sandwich cylindrical panel for $I_1 = I_2 = I_3 = I_4 = I_5 = 5$: present analysis (–) and Brischetto and Carrera (◯).

The described algorithm was performed with the Symbolic Math Toolbox, which incorporates symbolic computations into the numeric environment of MATLAB. This gives an opportunity to derive the exact 3D solutions of the heat conduction problem for laminated orthotropic cylindrical panels with a specified accuracy.

6.1. Two-layer cross-ply cylindrical panel

A two-layer cross-ply cylindrical panel with the stacking sequence [0/90] and ply thicknesses $h_1 = h_2 = h/2$ is composed of the graphite-epoxy composite considered in Section 5.1. To compare derived results with an approximate solution (Brischetto and Carrera, 2011) based on the fourth-order layer-wise theory (Carrera, 2003), we take $R = 10$ m, $a = 1$ m and $b = 10\pi/3$ m. The shell is subjected to the sinusoidally distributed temperature on the top surface, while the bottom surface is maintained at the reference temperature:

$$\Theta^{[N]} = \Theta_0 \sin\frac{\pi\theta_1}{a} \sin\frac{\pi\theta_2}{b}, \quad \Theta^{[0]} = 0, \tag{35}$$

where $\Theta_0 = 1$K.

The data listed in Table 6 show that the SaS method permits us to find the exact 3D solution for the thermal laminated orthotropic cylindrical panel with a prescribed accuracy by using the sufficiently large number of SaS. Fig. 4 presents the distributions of the temperature and heat flux in the thickness direction for different values of the slenderness ratio R/h employing eleven SaS for each layer. It is seen that both solutions agree well except for the outer layer in which the small difference can be observed in the case of $R/h = 10$.

Table 6
Temperature rise at the center of a two-layer cross-ply cylindrical panel at $z = 0.4$.

R/h	10	20	50	100	1000
$I_n = 3$	0.40741	0.51335	0.70887	0.82798	0.89917
$I_n = 5$	0.13005	0.37861	0.68458	0.82322	0.89913
$I_n = 7$	0.14158	0.38082	0.68466	0.82322	0.89913
$I_n = 9$	0.14535	0.38100	0.68466	0.82322	0.89913
$I_n = 11$	0.14509	0.38100	0.68466	0.82322	0.89913
$I_n = 13$	0.14508	0.38100	0.68466	0.82322	0.89913
$I_n = 15$	0.14508	0.38100	0.68466	0.82322	0.89913

6.2. Sandwich cylindrical panel

Finally, we consider a sandwich cylindrical panel with the stacking sequence [0/90/core/90/0] and ply thicknesses $h_1 = h_2 = h_4 = h_5 = 0.1\,h$ and $h_3 = 0.6\,h$. The face sheets are made of the two-ply graphite-epoxy composite with material properties given

Table 7
Temperature rise at the center of a sandwich cylindrical panel at z = 0.4.

R/h	10	20	50	100	1000
$I_n = 3$	0.33748	0.56899	0.85380	0.93856	0.97188
$I_n = 5$	0.33859	0.56904	0.85380	0.93856	0.97188
$I_n = 7$	0.33859	0.56904	0.85380	0.93856	0.97188

in Section 5.1. The thermal conductivities of the core are taken as $k_{11} = k_{22} = k_{33} = 0.18$ W/mK. The geometric parameters are chosen to be $R = 10$ m, $a = 1$ m and $b = 10\pi/3$ m (Brischetto and Carrera, 2011). The shell is subjected to temperature loading according to (35).

Table 7 demonstrates the results of the convergence study utilizing a various number of SaS I_n inside the nth layer. Fig. 5 displays the through-thickness distributions of the temperature and heat flux for the different slenderness ratios R/h employing five SaS for each layer. As can be seen, the continuity conditions for the heat flux at interfaces are satisfied again properly by using the constitutive Eq. (16).

7. Conclusions

An efficient approach of solving the 3D steady-state heat conduction problem for laminated orthotropic and anisotropic shells has been proposed. It is based on the new method of SaS parallel to the middle surface and located at Chebyshev polynomial nodes inside the individual layers and interfaces as well. The heat conduction analysis of laminated shells is based on the Fourier's constitutive equations and gives the possibility to obtain the exact 3D solutions for thick and thin thermal laminated cross-ply and angle-ply shells with a prescribed accuracy.

Acknowledgement

This work was supported by Russian Ministry of Education and Science under Grant No. 1.472.2011 and by Russian Foundation for Basic Research under Grant No. 13-01-00155.

References

Akhras, G., Li, W.C., 2007. Three-dimensional static, vibration and stability analysis of piezoelectric composite plates using a finite layer method. Smart Materials and Structures 16, 561–569.
Akhras, G., Li, W.C., 2010. Three-dimensional thermal buckling analysis of piezoelectric antisymmetric angle-ply laminates using finite layer method. Composite Structures 92, 31–38.
Brischetto, S., 2009. Effect of the through-the-thickness temperature distribution on the response of layered and composite shells. International Journal of Applied Mechanics 1, 1–25.
Brischetto, S., Carrera, E., 2011. Heat conduction and thermal analysis in multilayered plates and shells. Mechanics Research Communications 38, 449–455.
Burden, R.L., Faires, J.D., 2010. Numerical Analysis, ninth ed. Brooks/Cole, Cengage Learning, Boston.
Carrera, E., 2003. Theories and finite elements for multilayered plates and shells: a unified compact formulation with numerical assessment and benchmarking. Archives of Computational Methods in Engineering 10, 215–296.
Cheung, Y.K., Jiang, C.P., 2001. Finite layer method in analyses of piezoelectric composite laminates. Computer Methods in Applied Mechanics and Engineering 191, 879–901.
Kapuria, S., Sengupta, S., Dumir, P.C., 1997. Three-dimensional solution for a hybrid cylindrical shell under axisymmetric thermoelectric load. Archive of Applied Mechanics 67, 320–330.
Kulikov, G.M., 2001. Refined global approximation theory of multilayered plates and shells. Journal of Engineering Mechanics 127, 119–125.
Kulikov, G.M., Carrera, E., 2008. Finite deformation higher-order shell models and rigid-body motions. International Journal of Solids and Structures 45, 3153–3172.
Kulikov, G.M., Plotnikova, S.V., 2011a. Solution of statics problems for a three-dimensional elastic shell. Doklady Physics 56, 448–451.
Kulikov, G.M., Plotnikova, S.V., 2011b. On the use of a new concept of sampling surfaces in shell theory. Advanced Structured Materials 15, 715–726.
Kulikov, G.M., Plotnikova, S.V., 2012a. A method of solving three-dimensional problems of elasticity for laminated composite plates. Mechanics of Composite Materials 48, 23–36.
Kulikov, G.M., Plotnikova, S.V., 2012b. Exact 3D stress analysis of laminated composite plates by sampling surfaces method. Composite Structures 94, 3654–3663.
Kulikov, G.M., Plotnikova, S.V., 2012c. On the use of sampling surfaces method for solution of 3D elasticity problems for thick shells. ZAMM – Journal of Applied Mathematics and Mechanics 92, 910–920.
Kulikov, G.M., Plotnikova, S.V., 2013a. Three-dimensional exact analysis of piezoelectric laminated plates via sampling surfaces method. International Journal of Solids and Structures 50, 1916–1929.
Kulikov, G.M., Plotnikova, S.V., 2013b. Advanced formulation for laminated composite shells: 3D stress analysis and rigid-body motions. Composite Structures 95, 236–246.
Kulikov, G.M., Plotnikova, S.V., 2013c. A sampling surfaces method and its application to three-dimensional exact solutions for piezoelectric laminated shells. International Journal of Solids and Structures 50, 1930–1943.
Liew, K.M., Ng, T.Y., Zhang, J.Z., 2002. Differential quadrature-layerwise modeling technique for the three-dimensional analysis of cross-ply laminated plates of various edge-supports. Computer Methods in Applied Mechanics and Engineering 191, 3811–3832.
Liew, K.M., Zhang, J.Z., Ng, T.Y., Meguid, S.A., 2003. Three-dimensional modelling of elastic bonding in composite laminates using layerwise differential quadrature. International Journal of Solids and Structures 40, 1745–1764.
Malekzadeh, P., 2009. A two-dimensional layerwise-differential quadrature static analysis of thick laminated composite circular arches. Applied Mathematical Modelling 33, 1850–1861.
Malekzadeh, P., Farid, M., Zahedinejad, P., 2008. A three-dimensional layerwise-differential quadrature free vibration analysis of laminated cylindrical shells. International Journal of Pressure Vessels and Piping 85, 450–458.
Noor, A.K., Burton, W.S., 1992. Computational models for high-temperature multilayered composite plates and shells. Applied Mechanics Reviews 45, 419–446.
Reddy, J.N., 2004. Mechanics of Laminated Composite Plates and Shells: Theory and Analysis, 2nd ed. CRC Press, Boca Raton.
Savoia, M., Reddy, J.N., 1995. Three-dimensional thermal analysis of laminated composite plates. International Journal of Solids and Structures 32, 593–608.
Setoodeh, A.R., Tahani, M., Selahi, E., 2011. Hybrid layerwise-differential quadrature transient dynamic analysis of functionally graded axisymmetric cylindrical shells subjected to dynamic pressure. Composite Structures 93, 2663–2670.
Soldatos, K.P., Ye, J.Q., 1995. Stationary thermoelastic analysis of thick cross-ply laminated cylinders and cylindrical panels. Acta Mechanica 110, 1–18.
Tauchert, T.R., Ashida, F., Noda, N., Adali, S., Verijenko, V., 2000. Developments in thermopiezoelasticity with relevance to smart composite structures. Composite Structures 48, 31–38.
Tungikar, V.B., Rao, K.M., 1994. Three dimensional exact solution of thermal stresses in rectangular composite laminate. Composite Structures 27, 419–430.
Vel, S.S., Batra, R.C., 2001. Generalized plane strain thermoelastic deformation of laminated anisotropic thick plates. International Journal of Solids and Structures 38, 1395–1414.
Vel, S.S., Batra, R.C., 2003. Generalized plane strain thermopiezoelectric analysis of multilayered plates. Journal of Thermal Stresses 26, 353–377.
Wu, C.P., Chang, Y.T., 2012. A unified formulation of RMVT-based finite cylindrical layer methods for sandwich circular hollow cylinders with an embedded FGM layer. Composites Part B 43, 3318–3333.
Wu, C.P., Kuo, C.H., 2013. A unified formulation of PVD-based finite cylindrical layer methods for functionally graded material sandwich cylinders. Applied Mathematical Modelling 37, 916–938.
Wu, C.P., Li, H.Y., 2010. The RMVT- and PVD-based finite layer methods for the three-dimensional analysis of multilayered composite and FGM plates. Composite Structures 92, 2476–2496.
Zhang, J.Z., Ng, T.Y., Liew, K.M., 2003. Three-dimensional theory of elasticity for free vibration analysis of composite laminates via layerwise differential quadrature modelling. International Journal for Numerical Methods in Engineering 57, 1819–1844.